Electronic Supplementary Material (ESI) for Sustainable Energy & Fuels.
This journal is © The Royal Society of Chemistry 2021

Supporting Information (SI) for: Constructing Ni/MoN Heterostructure Nanorod Arrays Anchored on Ni Foam for Efficient Hydrogen Evolution Reaction under Alkaline Condition

Jian-Hang Sun, Fei-Fan Guo*, Xuan-Yi Li, Jin Yang and Jian-Fang Ma*

Key Laboratory of Polyoxometalate and Reticular Material Chemistry of Ministry of Education, Faculty of Chemistry, Northeast Normal University, 5628 Renmin Street, Changchun 130024, China

Experimental

1. Synthesis of $NiMoO_4$@NF nanorods

The $NiMoO_4$ nanorods were hydrothermally grown on Ni foam ($NiMoO_4$@NF) according to the literature method[1]. Typically, $Ni(NO_3)_2 \cdot 6H_2O$ (0.35 g, 1.2 mmol) and $NaMoO_4 \cdot 2H_2O$ (0.32 g, 1.3 mmol) were dissolved in 30 mL deionized water and stirred until a transparent solution was achieved. The Ni foam was cut into 4×2 cm^2 pieces and cleaned in 3 M HCl solution and deionized water successively. The resulting solution was transferred into a 50 mL Teflon-lined stainless-steel autoclave. Then the Ni foam was soaked in the solution. The autoclave was heated at 150 ^oC and kept 6 h. After the reaction, the solution was removed, and the Ni foam was washed with ethanol and dried to obtain $NiMoO_4$@NF nanorods.

2. Synthesis of heterostructural Ni–MoN on Ni foam (Ni–MoN@NF)

Three pieces of the obtained 4×2 cm^2 $NiMoO_4$@NF nanorods were placed in a tube furnace, and 0.4 g of dicyandiamide was placed on the upstream side. The final catalyst was achieved after the sample was treated at 550 ^oC for 2 h with a heating rate

of 5 °C min^{-1} under Ar atmosphere. For comparison, the catalysts that were treated at 500, 550 and 600 °C were named as Ni–MoN@NF500, Ni–MoN@NF550 and Ni–MoN@NF600, respectively. To study the influence of the amount of dicyandiamide on the performance of the catalyst, 0.1, 0.2, 0.3, 0.4, 0.5 and 0.6 g of dicyandiamide were used, respectively, under the same condition. The prepared target catalysts were called as Ni–MoN@NF0.1, Ni–MoN@NF0.2, Ni–MoN@NF0.3, Ni–MoN@NF0.4, Ni–MoN@NF0.5 and Ni–MoN@NF0.6, respectively.

3. Synthesis of MoN@NF

The MoN@NF sample was achieved by immersing the Ni–MoN@NF composite in 3 M HCl to remove metal Ni.

4. Synthesis of NiMo–H@NF

Three pieces of the obtained $NiMoO_4$@NF were placed in a tube furnace. The final NiMo–H@NF nanorods were obtained after the sample was treated at 550 °C for 2 h with a heating rate of 5 °C min^{-1} under 5% H_2/Ar atmosphere.

5. Physical Characterization

Powder X-ray diffraction (PXRD) patterns were determined on MiniFlex600-C X-ray diffractometer. The microstructure and morphology were analyzed by Field emission scanning electron microscopy (FESEM, FEI Tecnai F-20) and high-resolution transmission electron microscopy (HR-TEM, Hillsboro, OR, USA). X-ray photoelectron spectrometer (Thermo ESCALAB 250) was utilized to analyze the surface elemental composition and valence bond structure.

6. Electrochemical measurements

The HER performance of the electrocatalysts was tested with a typical three-electrode system in 1 M KOH by using an electrochemical workstation (CHI760E, China). A piece of sample with an area of 0.5×0.5 cm^2 was directly used as the working electrode. For comparative purposes, 3 mg of commercially available 20 wt% Pt/C was bonded on the same area of NF by using Nafion. A saturated Hg/HgO electrode and a

graphite rod were used as the reference and counter electrodes, respectively. The potential referred in this work was converted according to the equation $E_{RHE} = E_{Hg/HgO} + 0.098 + 0.059 \times pH$. The linear sweep voltammetry (LSV) was tested from 0 to −0.4 V *vs.* RHE with 5 mV s^{-1}. Tafel curves were calculated from LSV. Electrochemical impedance spectroscopy (EIS) was implemented from 100 kHz to 100 mHz with AC amplitude of 5 mV. The long-term cycling test was conducted for 2000 times at the potentials between 0.1 and 0.3 V *vs.* RHE with 50 mV s^{-1} and the V-t curve was also collected at a controlled current density of −10 mA cm^{-2} for 100 h.

The electrochemically capacitance (C_{dl}) and the Electrochemically Active Surface Area (A_{ECSA}) are linearly proportional. Therefore, the A_{ECSA} can be estimated by the C_{dl}, which can be easily conducted by cyclic voltammograms in the region of 0.02 to 0.13 V at various scan rates (10, 20, 30, 40, 50, 60, 70, 80, 90 and 100mV s^{-1}). The capacitance was calculated in a potential where no faradic processes were observed, *i.e.,* at 0.05 V *vs.* RHE. And the slope of the Δj vs. scan rate curve is twice that of the C_{dl}. According to the previous report, it is suitable that using a 40 μF cm^{-2} as the specific capacitance value. Thus, the A_{ECSA} can be reckoned by the following formula[1]:

$$A_{ECSA} = \frac{Cdl}{40\ \mu F\ cm^{-2}} * A\ geo$$

where A_{ECSA} is the electrochemically active surface area, and Ageo is the geometric area of electrode.

The TOF values of the catalysts were calculated from the equation:

$$TOF = (J \times A)/(2 \times F \times n)$$

where J is the current density at a given overpotential, A is the surface area of the NF, F is the Faraday constant (96,485 C mol^{-1}), and n is the number of moles of the active sites of the catalyst deposited on the electrode.

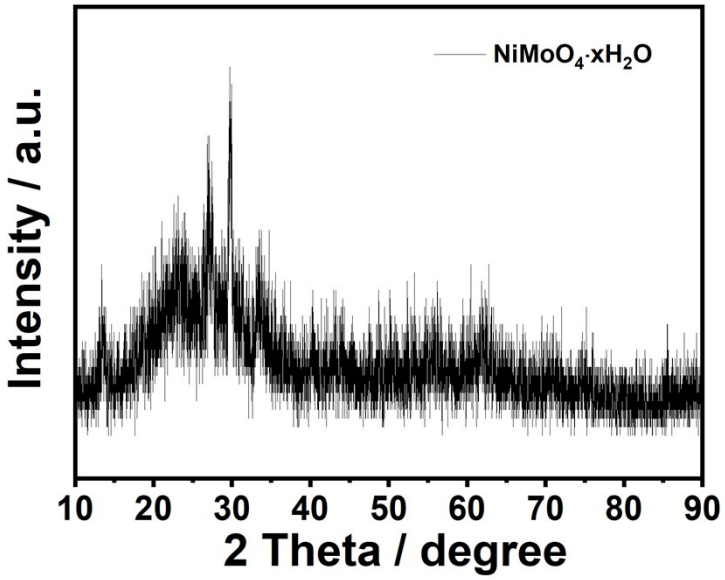

Figure S1. (a) XRD pattern of $NiMoO_4$ nanorods.

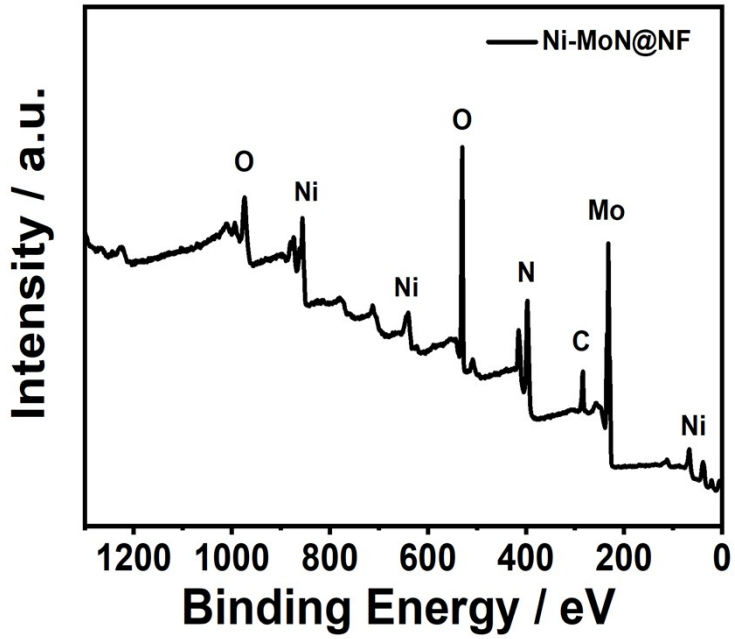

Figure S2. XPS full scan spectroscopy of Ni–MoN@NF.

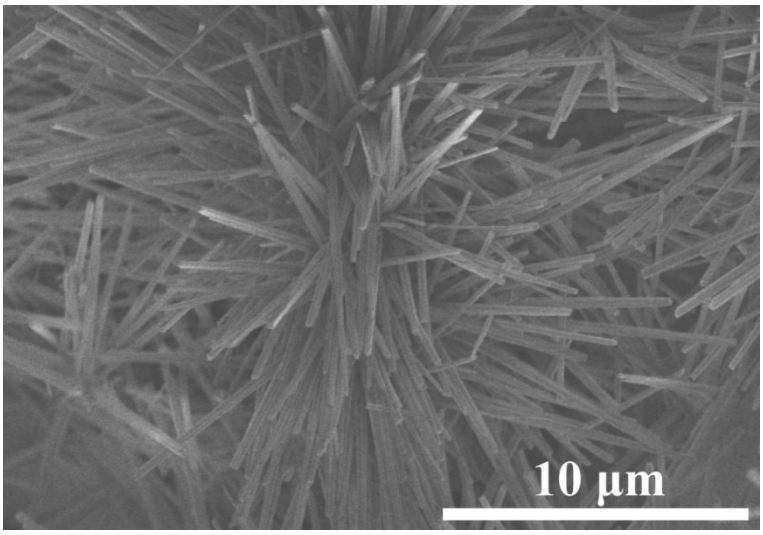

Figure S3. SEM images of $NiMoO_4$ nanorods.

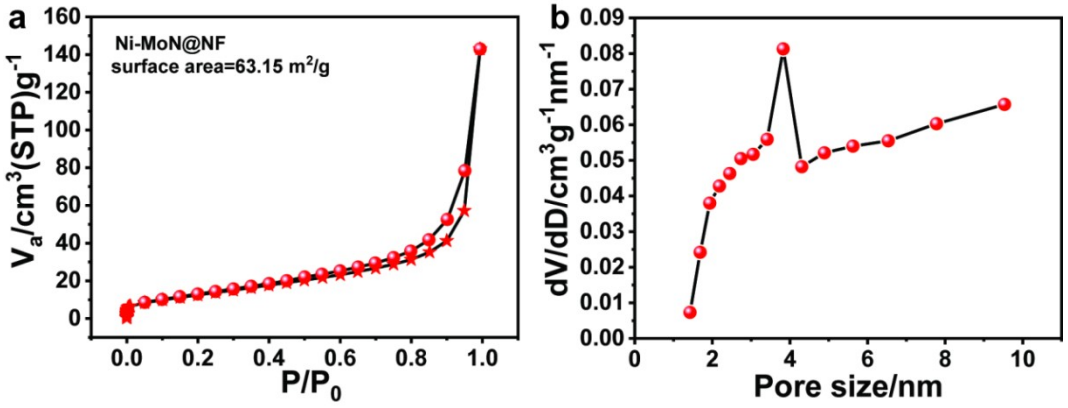

Figure S4. (a) N_2 adsorption-desorption isotherms and (b) BJH pore size distribution of Ni–MoN.

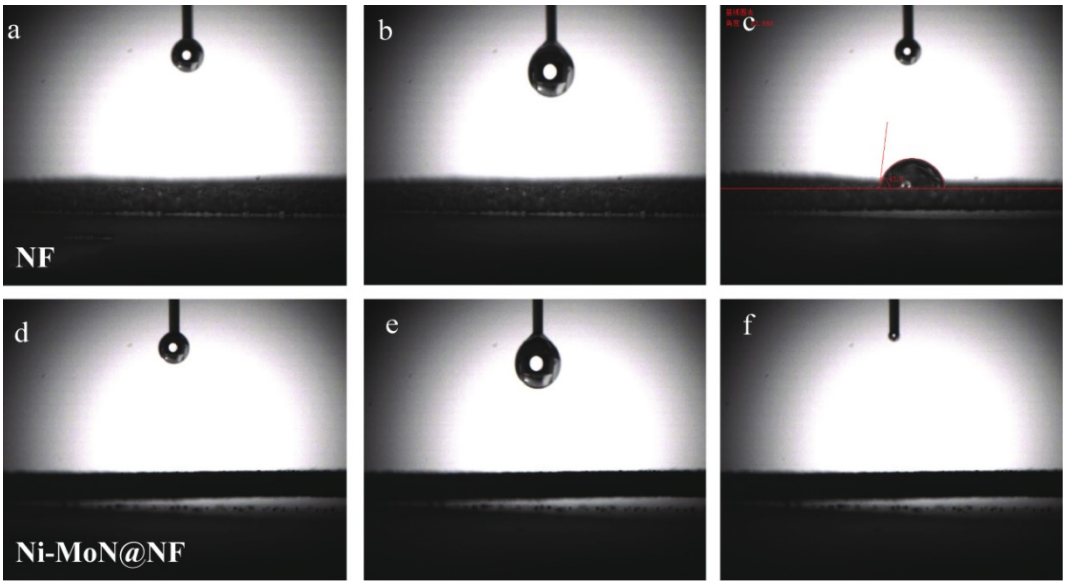

Figure S5. Examples of droplets for DI-water on (a-c) NF and (d-f) Ni–MoN@NF.

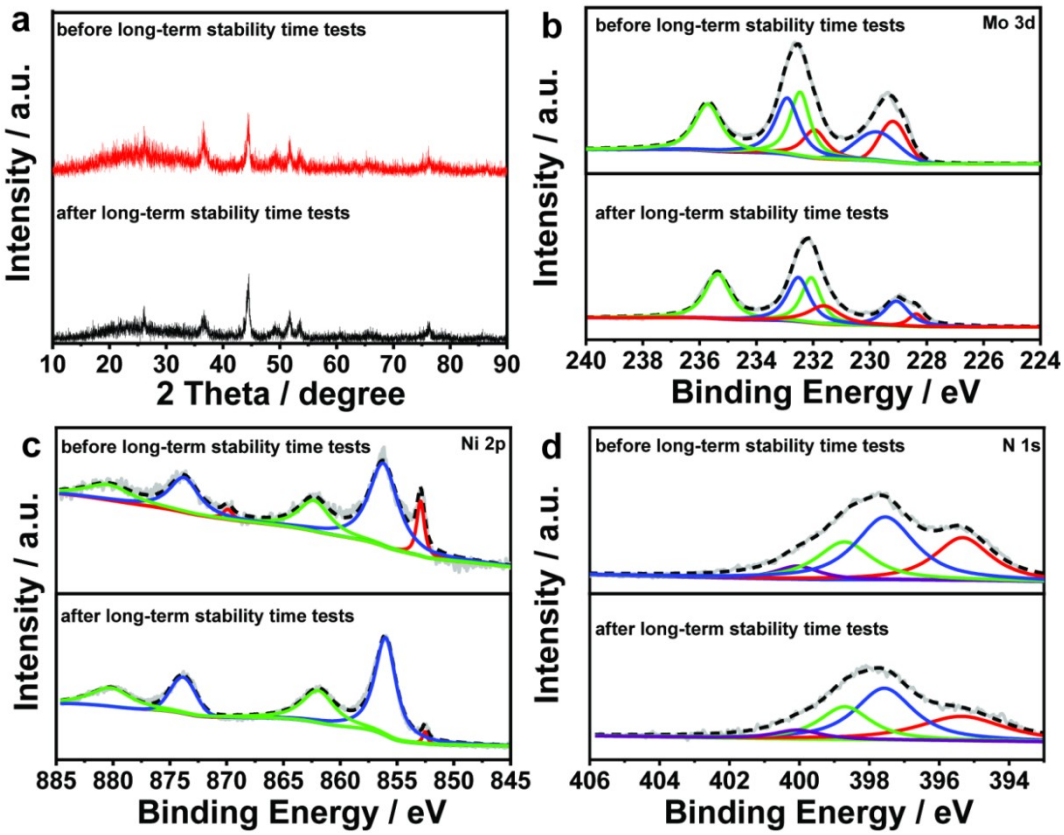

Figure S6. (a) XRD patterns of Ni–MoN@NF; High-resolution XPS spectra of Ni–MoN@NF (b) Mo 3d, (c) Ni 2p and (d) N 1s.

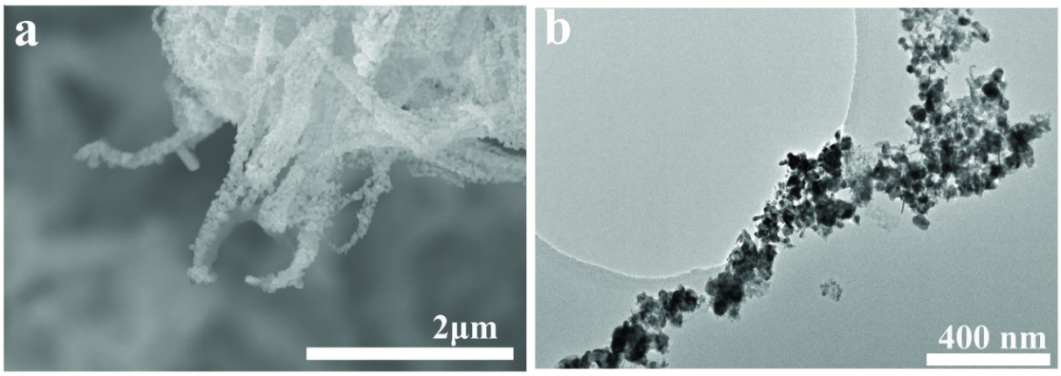

Figure S7. (a) SEM and (b) TEM images of Ni–MoN@NF after long-term stability time test.

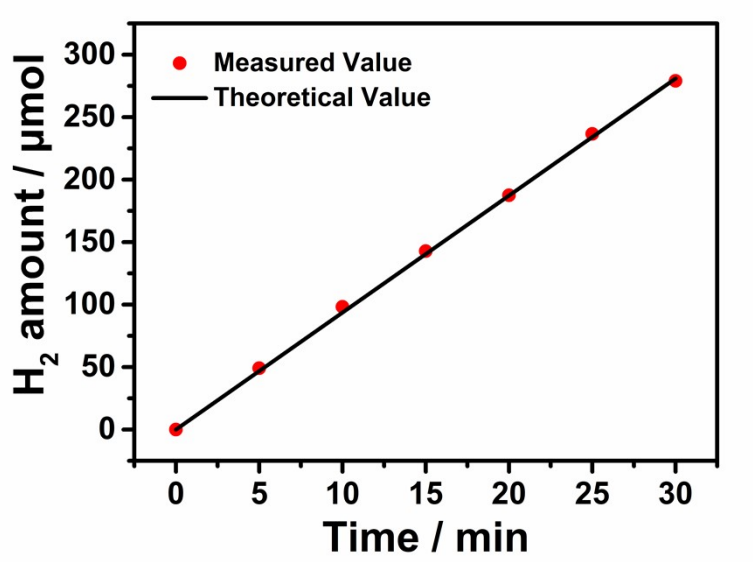

Figure S8. Comparison between theoretical calculation and experimental measurement of H_2 evolution, indicating an up to 100% FE for H_2 production on Ni–MoN@NF catalysts.

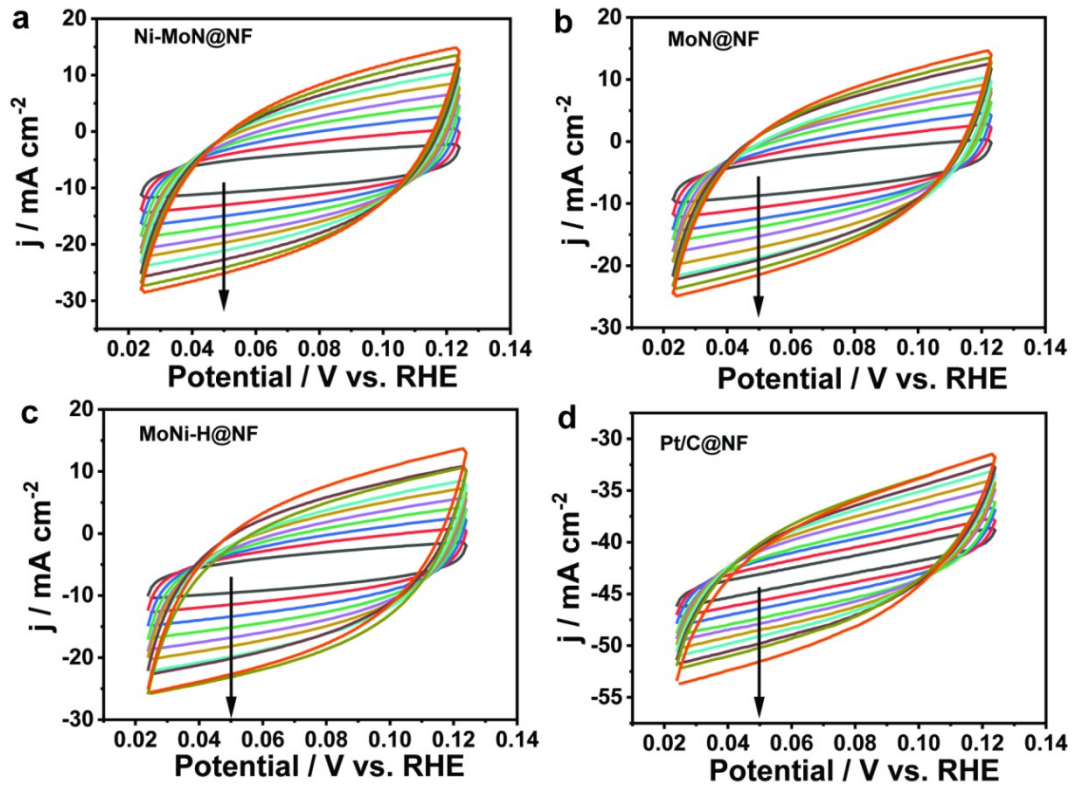

Figure S9. CVs with different rates from 10 to 100 mV s^{-1} in the region of 0.02-0.13 V for (a) Ni–MoN@NF, (b) MoN@NF, (c) MoNi–H@NF and (d) Pt/C@NF in 1 M KOH.

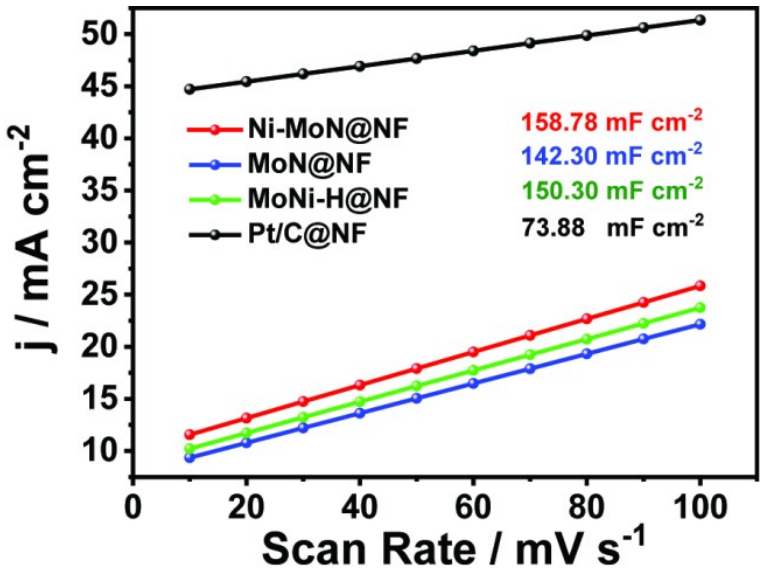

Figure S10. Double layer capacitance (C_{dl}) of Ni–MoN@NF, MoN@NF, MoNi–H@NF, and Pt/C@NF.

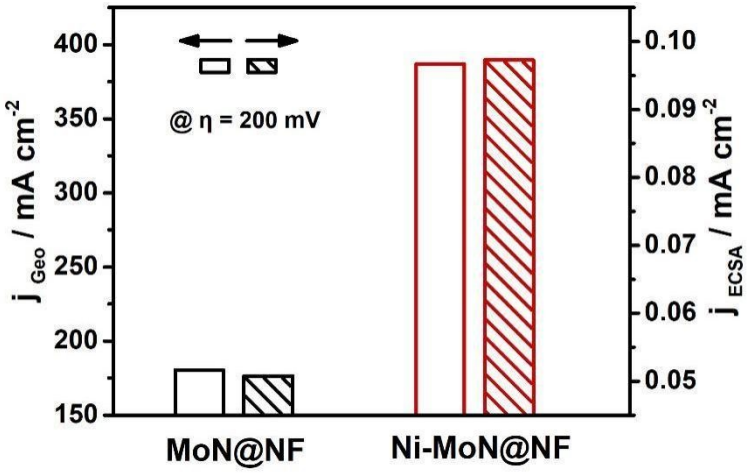

Figure S11. Comparison of the geometrical area and electrochemical active surface area (ECSA)-normalized specific activities of Ni–MoN@NF and MoN@NF, (evaluated at an overpotential of 200 mV).

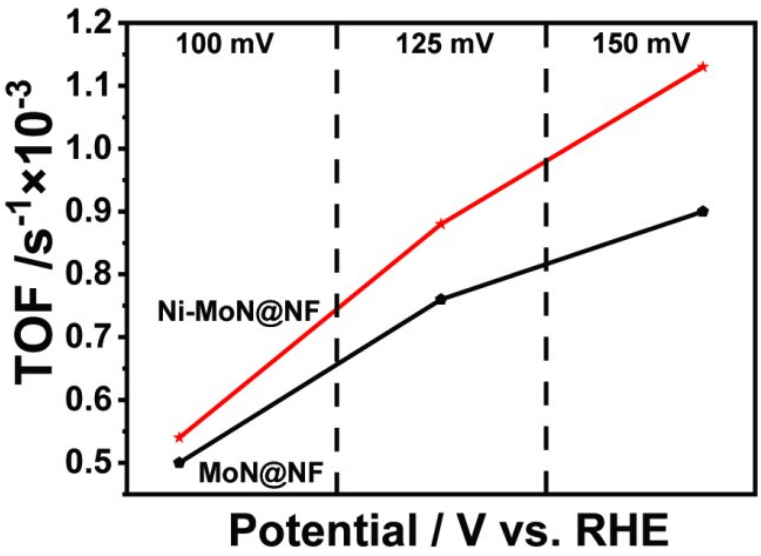

Figure S12 Turnover Frequencies of the resulting Ni–MoN@NF and MoN@NF at various current densities.

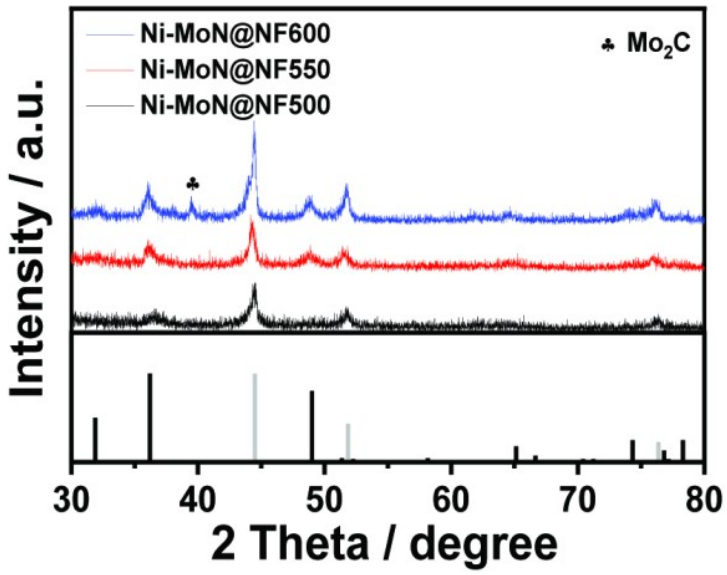

Figure S13. XRD patterns of Ni–MoN@NF500, Ni–MoN@NF550 and Ni–MoN@NF600.

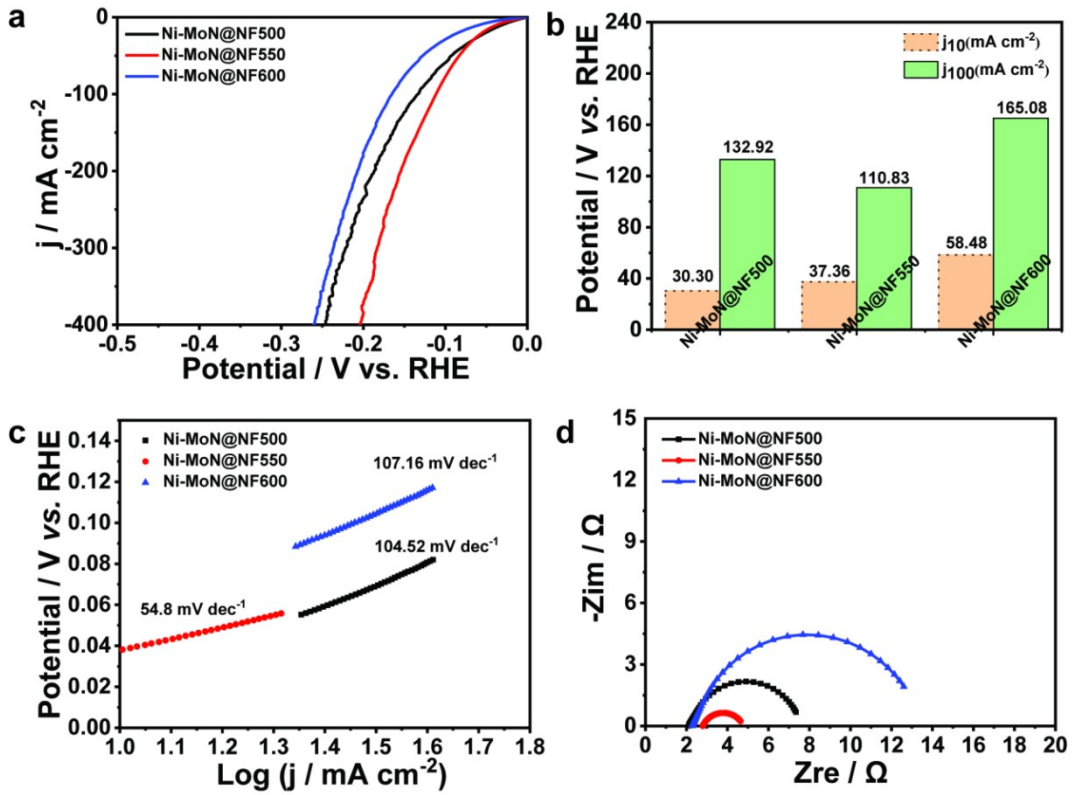

Figure S14. (a) Polarization curves; (b) histogram of overpotentials at 10 and 100 mA cm^{-2} for Ni–MoN@NF500, Ni–MoN@NF550, Ni–MoN@NF600 substrate measured in 1 M KOH; (c) corresponding Tafel plots; (d) electrochemical impedance spectra of Ni–MoN@NF500, Ni–MoN@NF550, Ni–MoN@NF600.

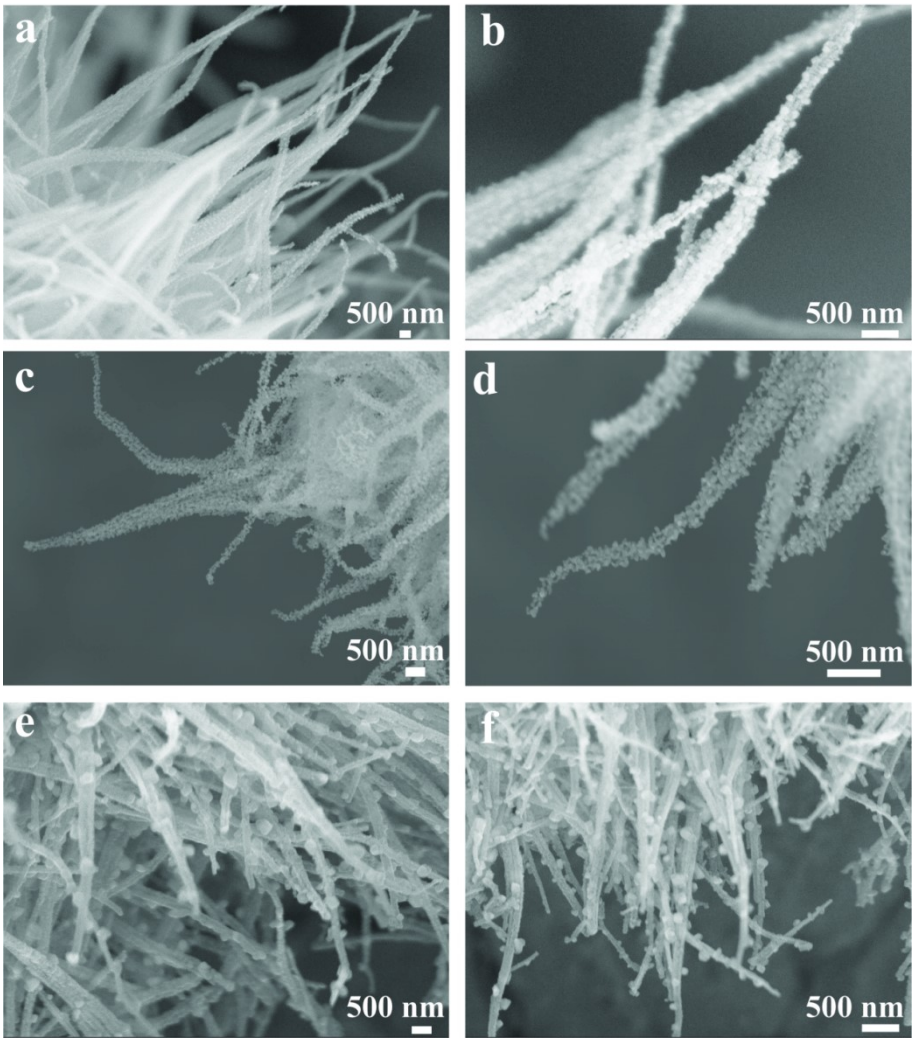

Figure S15. (a-b) SEM images of Ni–MoN@NF500; (c-d) SEM images of Ni–MoN@NF550; (e-f) SEM images of Ni–MoN@NF600.

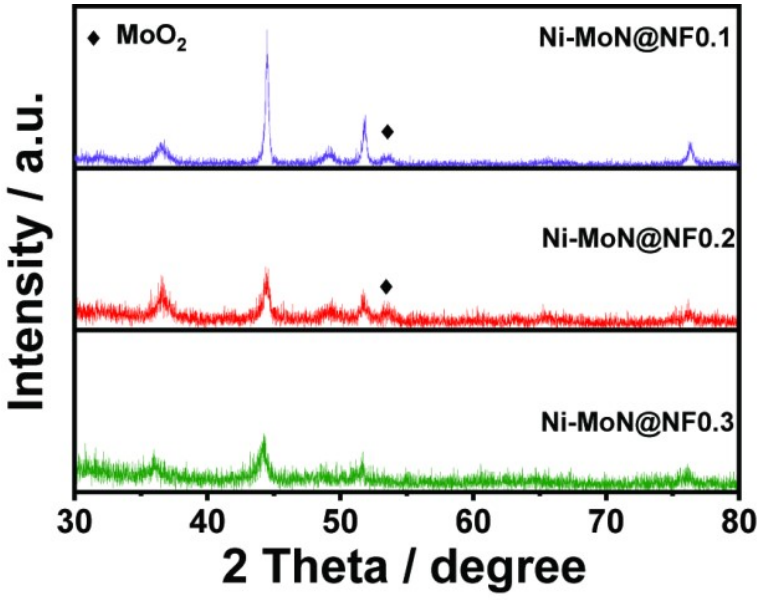

Figure S16. XRD patterns of Ni–MoN@NF0.1, Ni–MoN@NF0.2 and Ni–MoN@NF0.3.

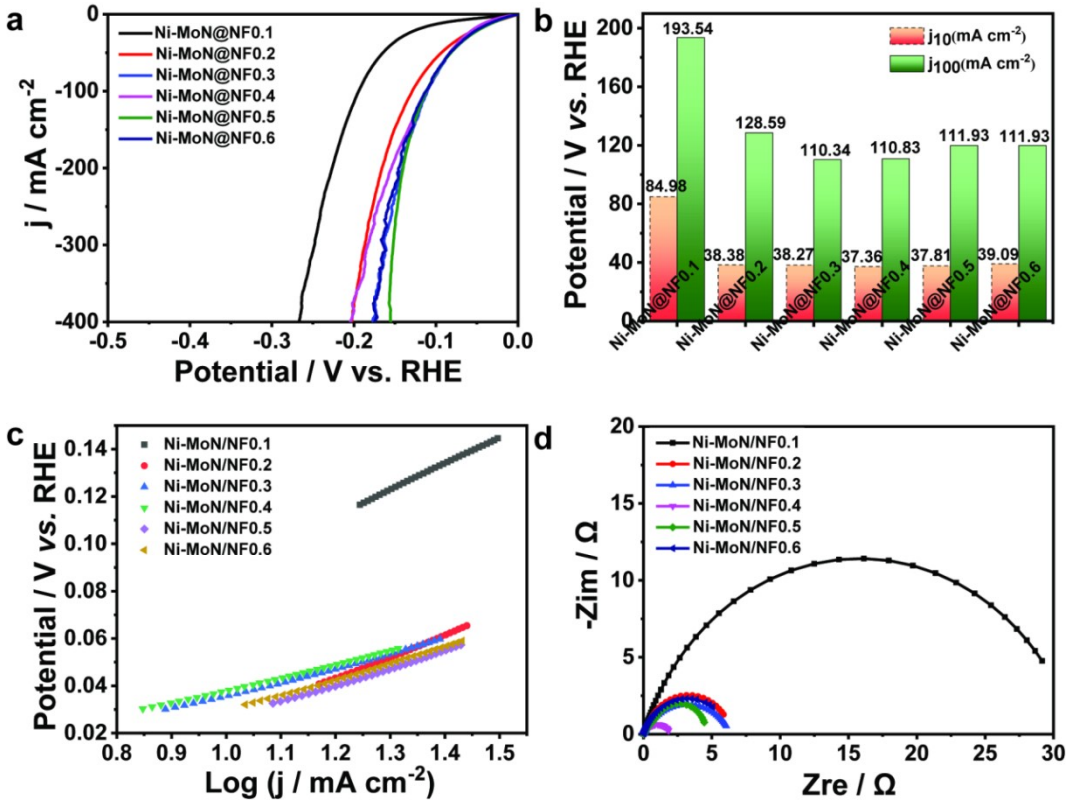

Figure S17. (a) Polarization curves; (b) histogram of overpotentials at 10 and 100 mA cm^{-2} for Ni–MoN@NF0.1－Ni–MoN@NF0.6; (c) corresponding Tafel plots; (d) electrochemical impedance spectra of Ni-MoN@NF0.1－Ni–MoN@NF0.6.

Table S1. Summary of state-of-the-art electrocatalysts in KOH for HER

Catalyst	Support	Electrolyte	η_{10} [mV]	Tafel slope [mV dec^{-1}]	Reference
Ni–MoN@NF	Ni foam	1 M KOH	37.36	57.6	This work
Ni−$Ni_{0.2}Mo_{0.8}N$	Ni foam	1 M KOH	15	39	ACS Appl. Mater. Interfaces, 2018, 10, 30400
Ni_3N-$Ni_{0.2}Mo_{0.8}N$ sheets	C foam	1 M KOH	31	64	Nano Energy, 2018, 44, 353
Ni-$Ni_{0.2}Mo_{0.8}N$particles	Glassy carbon	1 M KOH	38	40	Nano Energy, 2016, 22, 111
Ni/Ni_2P/Mo_2C@C	Glassy carbon	1 M KOH	223	68	J. Mater. Chem. A, 2018, 6, 5789
Ni-Mo_2C-CNF	Glassy carbon	1 M KOH	197	54.7	J. Colloid Interface Sci., 2020, 558, 100
MoS_2-Ni_3S_2 HNRs	Ni foam	1 M KOH	98	61	ACS Catal., 2017, 7, 2357
Co_2P/Mo_3Co_3C/Mo_2C@C	Glassy carbon	1 M KOH	182	65	J. Mater. Chem. A, 2018, 6, 5789
Ni_3N@VN	Ni foam	1 M KOH	56	47	J. Mater. Chem. A, 2019, 7, 5513
Ni_3N-VN	Ni foam	1 M KOH	64	37	Adv. Mater., 2019, 31, 1901174
NiMoN/NF-450	Ni foam	1 M KOH	22	101	J. Mater. Chem. A, 2018, 6, 8479
Ni-SN@C	Membrane	1 M KOH seawater	23	39	Adv. Mater., 2021, 2007508

[1] .Sun J, Liu J, Chen H, Han X, Wu Y, He J, et al. Strongly Coupled Mo_2C and Ni Nanoparticles with *in-situ* Formed Interfaces Encapsulated by Porous Carbon Nanofibers for Efficient Hydrogen Evolution Reaction under Alkaline Conditions[J]. Journal of Colloid and Interface Science. 2020;558:100-105.

[2] . Yu Z-Y, Duan Y, Gao M-R, Lang C-C, Zheng Y-R, Yu S-H. A One-Dimensional Porous Carbon-Supported Ni/Mo_2C Dual Catalyst for Efficient Water Splitting[J]. Chemical Science. 2017;8(2):968-973.